Electronic Supplementary Material (ESI) for Molecular Systems Design & Engineering.

Supporting information for: Active learning of polarizable nanoparticle phase diagrams for the guided design of triggerable self-assembling superlattices

Siva Dasetty,[†] Igor Coropceanu,[‡] Joshua Portner,[‡] Jiyuan Li,[†] Juan J. de Pablo,[†] Dmitri Talapin,[†,‡,¶] and Andrew L. Ferguson[*,†]

†*Pritzker School of Molecular Engineering, University of Chicago, Chicago, Illinois 60637*

‡*Department of Chemistry, University of Chicago, Chicago, Illinois 60637*

¶*James Franck Institute, University of Chicago, Chicago, Illinois 60637*

E-mail: andrewferguson@uchicago.edu

1 Trends in the assembly of 20-particle system compared with experiments

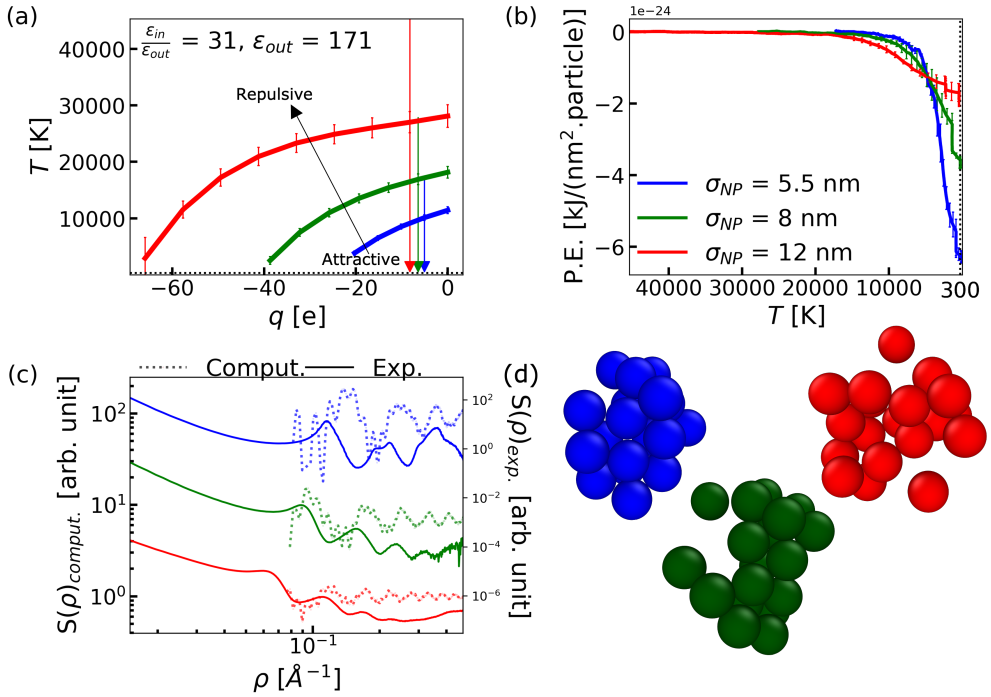

Figure S1: Computational and experimental comparison of the self-assembly of $K_4Sn_2S_6$ functionalized gold nanoparticles in NMF. (a) Calculated phase diagram for 2-particle assembly projected into the T-q plane for NPs of diameter σ_{NP} 5.5 nm (blue), 8 nm (green), and 12 nm (red). The lines correspond to the locus of points for which $\Delta A^* = 0$ separating the attractive and repulsive regimes are below and above each curve, respectively. Error bars on each phase boundary represent the standard deviation in ΔA^* estimated by the terminal fitted GPR model. The vertical arrows indicate the simulated annealing temperature quenches used to determine the stable self-assembled structures of our 20-particle systems from an initial high temperature down to the 300 K target temperature indicated by the horizontal dashed line. The location of each vertical arrow on the x-axis corresponds to the q value assigned to each NP in our simulations. (b) Potential energies (P.E.) (U_{NP-NP} in Eq. 1 (main text) normalized by particle surface area $4\pi(\sigma_{NP}/2)^2$ and number of particles) observed during the terminal temperature quench of the 20-particle simulated annealing calculations. (c) Comparison of computational (dotted) and experimental (solid) structure factors $S(\rho)$ for the terminal self-assembled aggregates. For clarity of viewing, the 5.5 nm (blue) experimental data are vertically shifted in log-scale by (−18.42) arb. unit and the 8 nm (green) data by (−6.50) arb. unit. The computational data are then aligned with the experimental results. To avoid confusion with our symbol for charge, we denote the scattering vector by ρ. (d) Snapshots of the self-assembled structures produced at the end of the simulated annealing calculations.

2 Computational design of temperature triggerable superlattices of particles with $\frac{\varepsilon_{in}}{\varepsilon_{out}}$ of 0.5

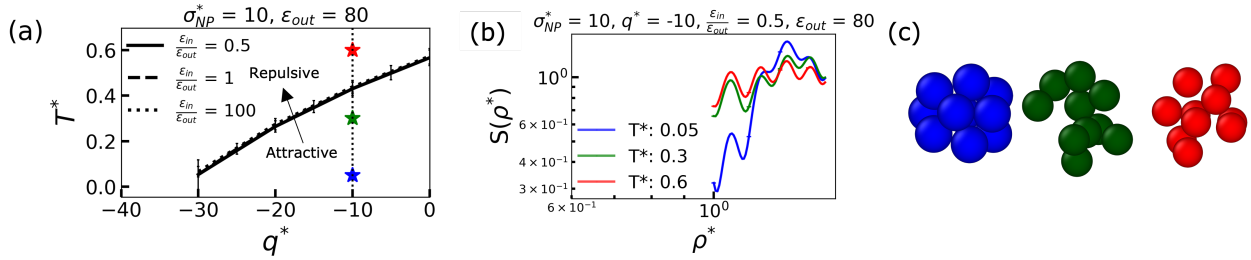

Figure S2: Computational design of temperature-triggerable assembly/disassembly in self-assembled NP superlattices. (a) Calculated phase diagram for 2-particle assembly projected into the T^*-q^* plane for NPs of diameter $\sigma^*_{NP} = 10$ in a solvent with a dielectric constant of $\varepsilon_{out} = 80$ and different dielectric contrasts $\frac{\varepsilon_{in}}{\varepsilon_{out}} = 0.5$, 1, and 100. The lines correspond to the locus of points for which $\Delta A^* = 0$ separating the attractive and repulsive regimes below and above each curve, respectively. Different line styles correspond to different $\frac{\varepsilon_{in}}{\varepsilon_{out}}$. Error bars on each phase boundary represent the standard deviation in ΔA^* estimated by the terminal fitted GPR model. The location of the vertical dotted line on the x-axis corresponds to the q value assigned to the NP in our simulations. The stars on the vertical dotted line represent the temperature at which structure analysis was performed – 0.05 (blue), 0.3 (green), and 0.6 (red). (b) Computed structure factors $S(\rho)$ for the terminal self-assembled aggregates at each temperature highlighted in (a) spanning across the phase boundary for $\frac{\varepsilon_{in}}{\varepsilon_{out}} = 0.5$. (c) Snapshots of the self-assembled structures corresponding to computed structure factors shown in (b) at each temperature.

3 Computational design of temperature triggerable superlattices of particles with $\frac{\varepsilon_{in}}{\varepsilon_{out}}$ of 1.0

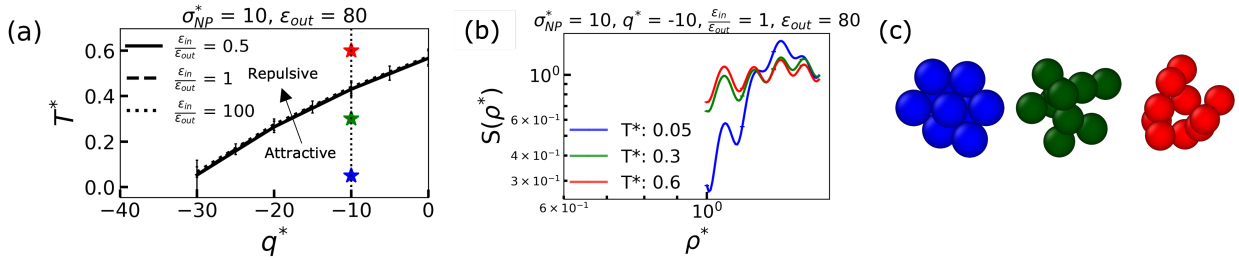

Figure S3: Computational design of temperature-triggerable assembly/disassembly in self-assembled NP superlattices. (a) Calculated phase diagram for 2-particle assembly projected into the T^*-q^* plane for NPs of diameter $\sigma^*_{NP} = 10$ in a solvent with a dielectric constant ε_{out} = 80 and different dielectric contrasts $\frac{\varepsilon_{in}}{\varepsilon_{out}} = 0.5$, 1, and 100. The lines correspond to the locus of points for which $\Delta A^* = 0$ separating the attractive and repulsive regimes are below and above each curve, respectively. Different line styles correspond to different $\frac{\varepsilon_{in}}{\varepsilon_{out}}$. Error bars on each phase boundary represent the standard deviation in ΔA^* estimated by the terminal fitted GPR model. The location of the vertical dotted line on the x-axis corresponds to the q value assigned to the NP in our simulations. The stars on the vertical dotted line represent the temperature at which structure analysis was performed – 0.05 (blue), 0.3 (green), and 0.6 (red). (b) Computed structure factors $S(\rho)$ for the terminal self-assembled aggregates at each temperature highlighted in (a) spanning across the phase boundary for $\frac{\varepsilon_{in}}{\varepsilon_{out}} = 1.0$. (c) Snapshots of the self-assembled structures corresponding to computed structure factors shown in (b) at each temperature.